Geophysical Investigation of Subsurface Structure at Biscuit Basin, Yellowstone National Park

Yuyang Dai

1. Introduction to the Problem

In the summer of 2024, a hydrothermal explosion occurred at Biscuit Basin in Yellowstone National Park. Although such events are not uncommon in hydrothermal terrains and are not necessarily indicative of renewed volcanism, this incident has drawn renewed scientific and public attention to the underlying subsurface processes. In particular, it has underscored the importance of geophysical imaging in constraining the distribution of fluids, gases, and heat within the shallow crust of the Yellowstone volcanic system.

To evaluate the structural and thermal conditions beneath the explosion site, the Yellowstone Volcano Observatory initiated a multi-method geophysical investigation. Active-source seismic data were collected using a linear array of 50 receivers spaced at 1 kilometer intervals along a 50 kilometers survey line. Arrival times of refracted and reflected P-waves were analyzed to determine subsurface seismic velocities and resolve layer interfaces. Concurrent gravity measurements along the same transect were used to model density contrasts and test for deep low-density zones possibly linked to magma or hydrothermal activity. Magnetic data were also acquired to map magnetization patterns and identify demagnetized regions. A block-based model was developed to match the anomaly and assess the extent of magnetic alteration beneath the line.

This report presents preliminary results from the seismic, gravity, and magnetic components of the survey. Velocity structures, density models, and magnetic signatures are interpreted to assess whether the explosion at Biscuit Basin reflects broader structural or magmatic processes within the Yellowstone hydrothermal system.

2. Background

Yellowstone National Park sits above one of the largest active magmatic hydrothermal systems in the world. Heat from a shallow magma chamber drives strong hydrothermal

activity. This is seen at the surface through geysers, steam vents, and hot springs. The subsurface contains layers of volcanic rock, altered zones, and glacial deposits. All of these rest on a high volcanic plateau (Fournier, 1989).

Hydrothermal explosions happened in Yellowstone's thermal areas. These events occur when steam builds up under a tight rock layer and then releases suddenly. The explosions can form craters and throw out large amounts of debris. While they are not always linked to deep magma, they still raise concern. The 2024 explosion at Biscuit Basin made us look into the flow of fluids, pressure buildup, and subsurface structure.

Geophysical methods are useful for studying the shallow crust. Seismic data can show changes in speed that point to different rock types. Gravity data help find places with low density that suggest magma. Magnetic data highlight areas that lost magnetism from heat. These areas often sit near active zones (Fournier, 1989; Morgan et al., 2009).

This study uses seismic data to estimate how fast waves move through the ground beneath Biscuit Basin. Gravity modeling is used to locate possible low-density regions. Magnetic modeling is used to detect demagnetized areas. Together, these methods offer a more complete picture of the shallow crust in the active hydrothermal regions.

3. Methods

3.1 Seismic Refraction

We used seismic refraction data from 50 geophones spaced 1 kilometer apart along a 50 kilometers line near Biscuit Basin. First-arrival P-waves from an active source were recorded. This method helps find changes in subsurface wave speed which often relate to changes in rock type.

To better match the data, we split the travel-time curve into three parts. Each part was fitted with a straight line using linear regression. This gave us three apparent wave speeds, each showing a different refracted phase from deeper layers.

This method does not rely on a single crossover point or two-layer model. It gives more detail by using multiple straight-line fits.

3.1.1 Strengths and Limitations:

Seismic refraction is good for mapping horizontal changes in wave speed and large layers near the surface. It works best when wave speeds get faster with depth. In this case, breaking the data into three parts gave decent detail about the subsurface. However, this method is not good at detecting dipping layers. For areas in Yellowstone with complex geology, the results can be unclear.

3.2 Seismic Reflection

Seismic reflection analysis was performed using four P-wave arrivals to estimate subsurface velocities and reflector depths. For each arrival, we applied a hyperbolic moveout model by plotting travel time squared (t^2) against distance squared (x^2) and fitting a line. The relationship follows the hyperbolic moveout equation:

$$t^2 = \frac{x^2}{v^2} + t_0^2 \quad (1)$$

Here, v is the reflection velocity and t_0 is the two-way zero-offset travel time. The slope of the fitted line provides $\frac{1}{v^2}$, and the intercept gives t_0^2. From these, we calculated both the velocity and the depth to each reflector using $h = v * \frac{t_0}{2}$.

To reduce intercept bias, we excluded the first few data points for each arrival and performed a linear regression on the remaining travel-time data.

3.2.1 Strengths and Limitations:

Seismic reflection is suited for detecting contrasts in acoustic velocity and imaging subsurface layering. It has high resolution where reflectors are continuous. However, reflection signals may be weakened in thermally altered zones which can make some interfaces difficult to interpret.

3.3 Gravity

Gravity data were collected along the same 50 kilometers profile as the seismic survey with 1 kilometer intervals. The goal was to identify subsurface density changes that might signal features like magma bodies. The observed gravity anomaly was modeled directly using forward simulation of rectangular prism blocks.

Two block models were created. They each with two bodies that represent different subsurface structures. The blocks were defined by their horizontal position, depth range, and assumed density contrast. We used the 'prism_gravity' function from Harmonica to calculate the vertical gravity component (g_z) across the grid. The gravity response was extracted along the center of the profile for comparison. Modeled results were evaluated using root mean square (RMS) error to measure the fit with the observed data.

3.3.1 Strengths and Limitations

Gravity method helps detect broad subsurface density changes. It works well for large features like magma chambers or hydrothermal buildup. However, gravity has limited ability to resolve shallow targets. Different subsurface structures can create similar signals which would make interpretation difficult. Reliable results often require support from seismic or geological information.

3.4 Magnetism

Magnetic anomaly data were collected along the same 50 kilometers survey line using 1 kilometer spacing. The goal was to map magnetization changes in the subsurface. These changes may point to thermal effects, magnetized bodies, or demagnetized zones.

We created a forward model using three prism blocks. Each block had a set position, depth, and vertical magnetization value. The blocks were assigned both positive and negative vertical magnetization values to simulate contrasting magnetic domains. We used Harmonica's 'prism_magnetic' tool to calculate the magnetic field over the model grid. The vertical field component (b_z) was extracted along the center of the profile.

The modeled result was compared to the observed data. Root mean square (RMS) misfit was used to measure the match. The final model reflects key features in the observed data and gives insight into subsurface magnetization.

3.4.1 Strengths and Limitations

Magnetic methods are useful for spotting thermal patterns in volcanic regions. They respond to both rock type and heat. But magnetic signals can weaken near the surface. Interpretation often improves when combined with seismic or geological input.

4. Results

4.1 Seismic Refraction Results

Refraction travel times were divided into three linear segments to better represent distinct velocity layers in the subsurface. Each segment was fit using linear regression, revealing a three-layer model:

- **Layer 1:** 4453 m/s (0 to 16.7 km)
- **Layer 2:** 5949 m/s (16.7 to 33.3 km)
- **Layer 3:** 6250 m/s (33.3 to 50 km)

No direct wave was identified in the dataset. All observed arrivals are interpreted as head waves refracted at increasing depths. The velocity increase with distance and depth is consistent with geologic layering.

Figure 1. Three-segment linear fit to refraction data. Each segment corresponds to head wave arrivals from a different subsurface layer.

4.2 Seismic Reflection

We applied linear fits to four reflected P-wave arrivals using the hyperbolic moveout equation. The analysis gave the following velocity and depth estimates:

- **Reflector 1:** v ≈ 2700 m/s, depth ≈ 385 m
- **Reflector 2:** v ≈ 3780 m/s, depth ≈ 2119 m
- **Reflector 3:** v ≈ 4712 m/s, depth ≈ 4911 m
- **Reflector 4:** v ≈ 5387 m/s, depth ≈ 7984 m

Each reflector was identified from a distinct travel-time curve. We plotted travel time squared (t^2) against distance squared (x^2) and used the slope and intercept to estimate both wave speed and layer depth. The slope provided the velocity, and the intercept was used to calculate depth. All four fits matched the observed data closely.

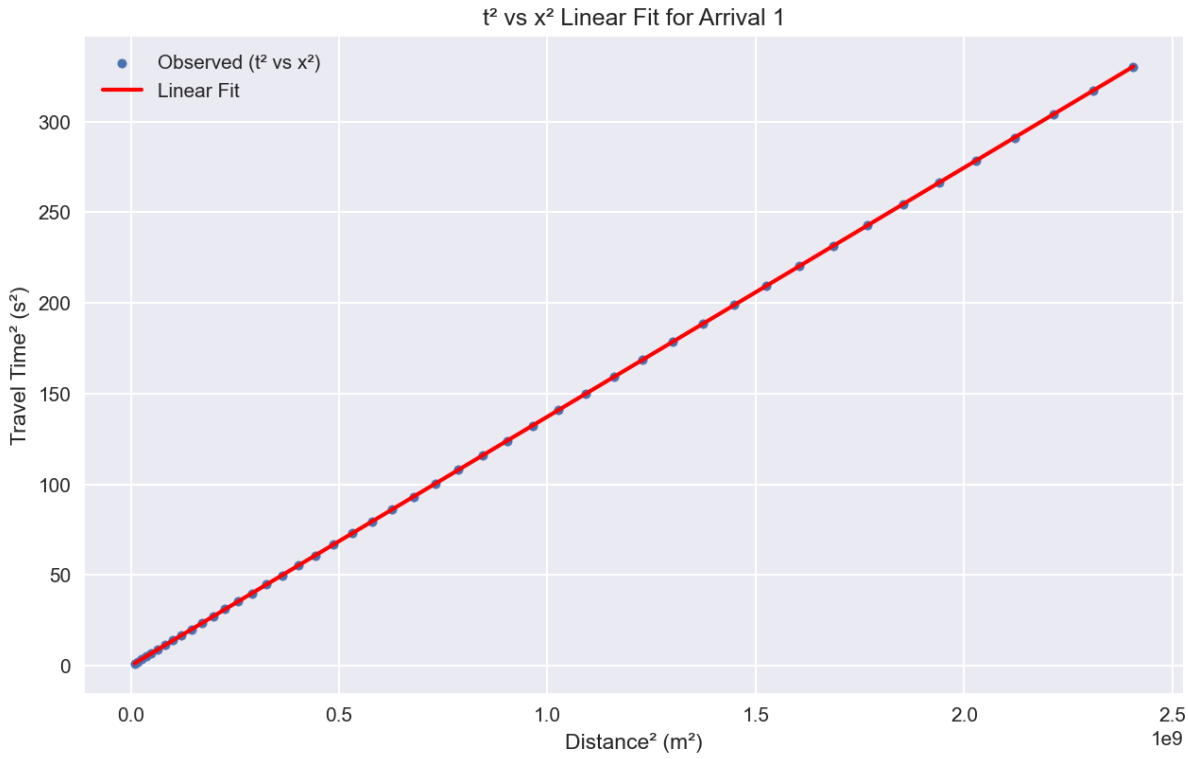

Figure 2. **Arrival 1.** Travel time squared plotted against offset squared with linear fit. The best-fit line shows strong alignment with observed data.

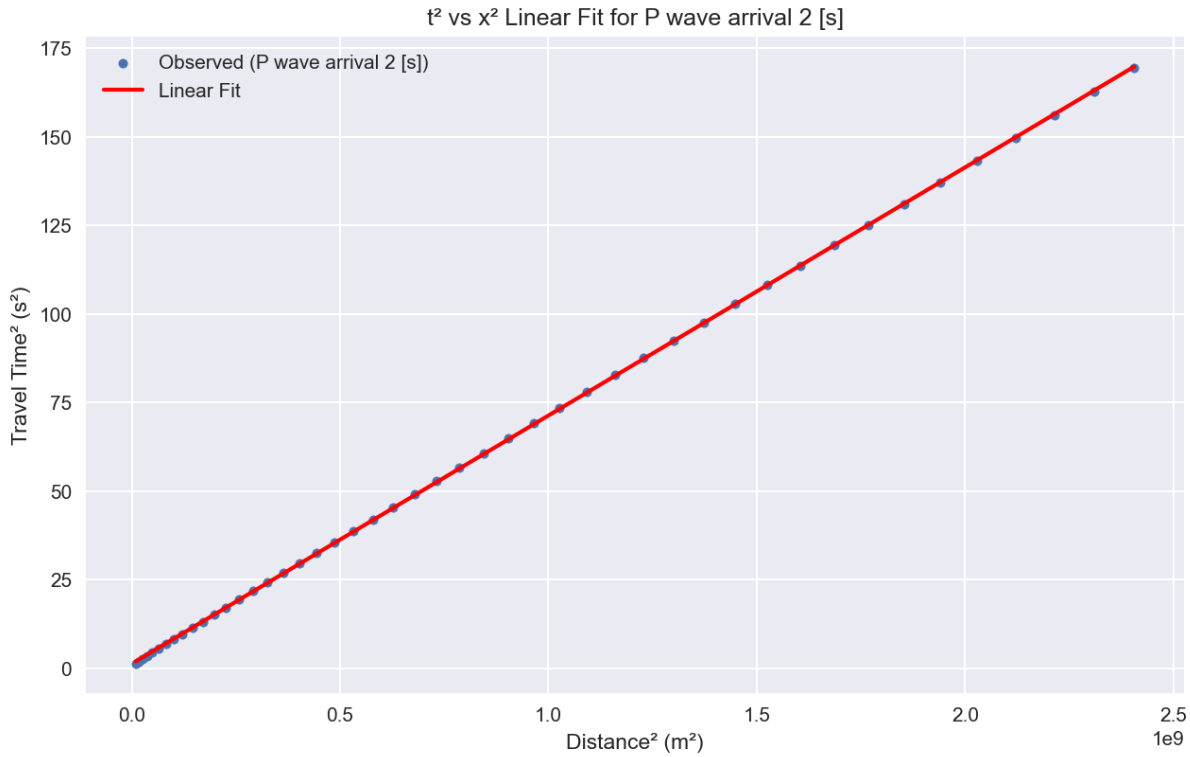

Figure 3. Arrival 2. Second reflection arrival showing consistent linear trend. Fit yields intermediate velocity and reflector depth.

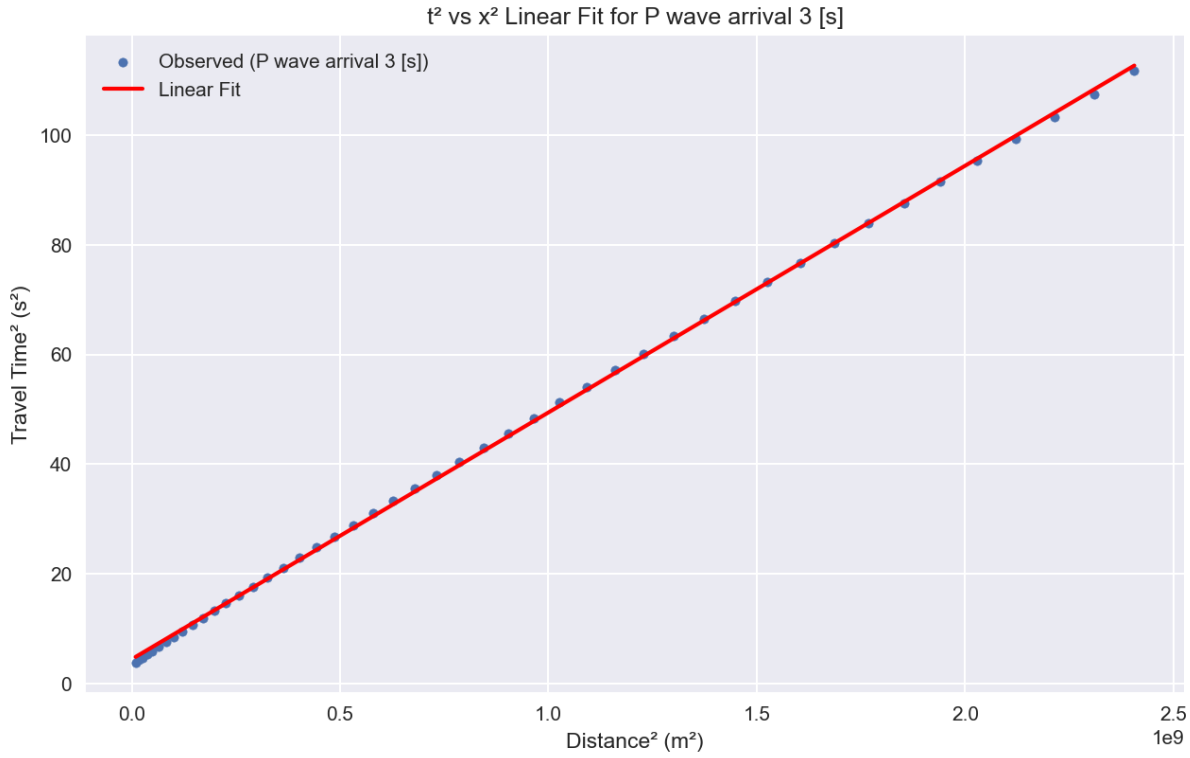

Figure 4. Arrival 3. Third reflection event with increased travel time. Fit indicates a deeper, higher-velocity interface.

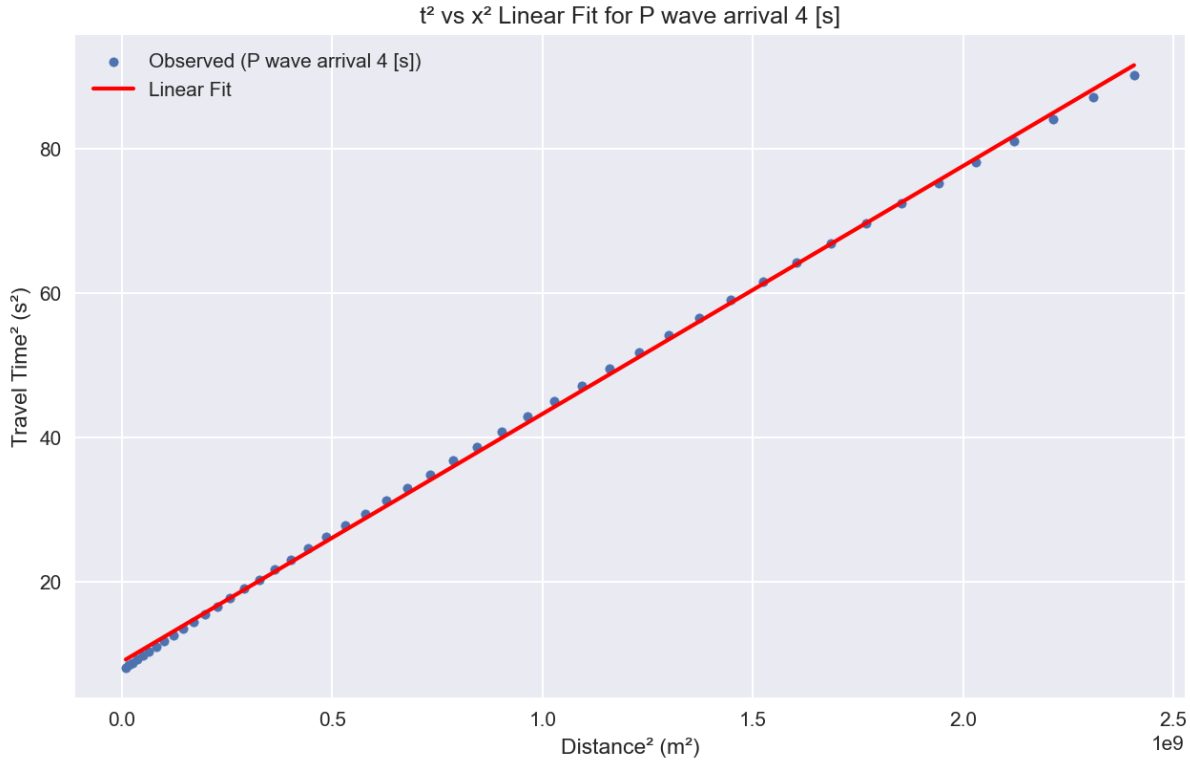

Figure 5. Arrival 4. Deepest identified reflector. Linear fit remains closely aligned with observed points, though slight deviation is visible at longer offsets.

4.2.1 Combined Seismic Velocity Model

We constructed a five-layer velocity model using results from both seismic reflection and refraction. Each layer is assigned a different color based on P-wave velocity. The shallowest zone starts at approximately 2700 m/s, and the deepest layer reaches about 6250 m/s.

The top four interfaces are based on reflection arrival depths: 385 m, 2110 m, 4910 m, and 7984 m. The bottom boundary at approximately 9 km depth is derived from the refraction analysis. Black triangles mark receiver locations at the surface, and the red triangle shows the explosion site at Biscuit Basin.

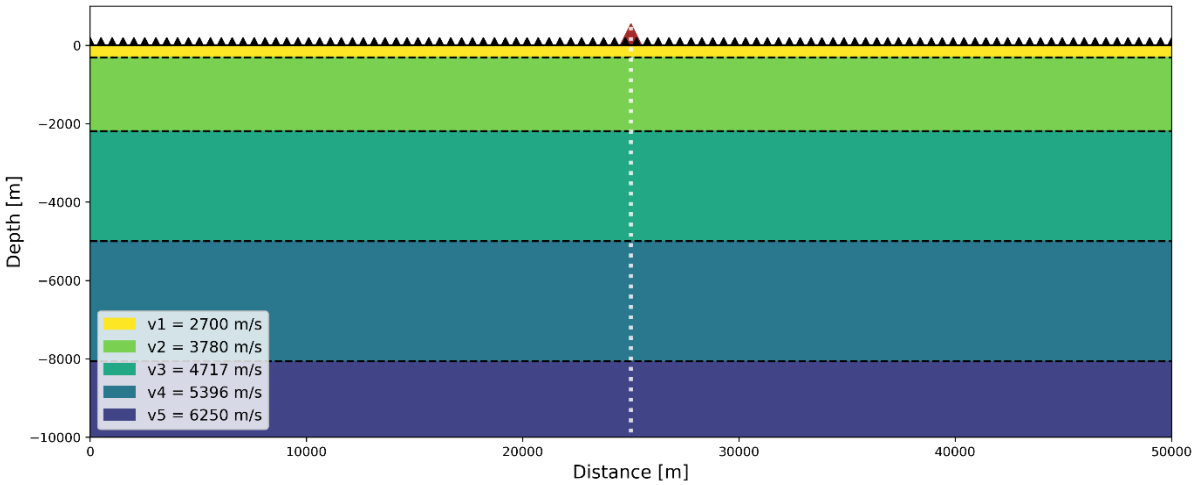

Figure 6. Conceptual five-layer velocity model derived from seismic reflection and refraction data. Colors represent increasing P-wave velocity with depth, from 2700 m/s to 6250 m/s.

4.3 Gravity Results

We created two gravity models using different block configurations. Each model produced a synthetic profile of the vertical gravity component. We compared both profiles to the observed data along the 50 kilometers survey line.

Model 1 shows a closer match in the central portion of the profile. Model 2 aligns more closely with the deeper low located near 40 km. The figure displays the observed anomaly along with both modeled curves.

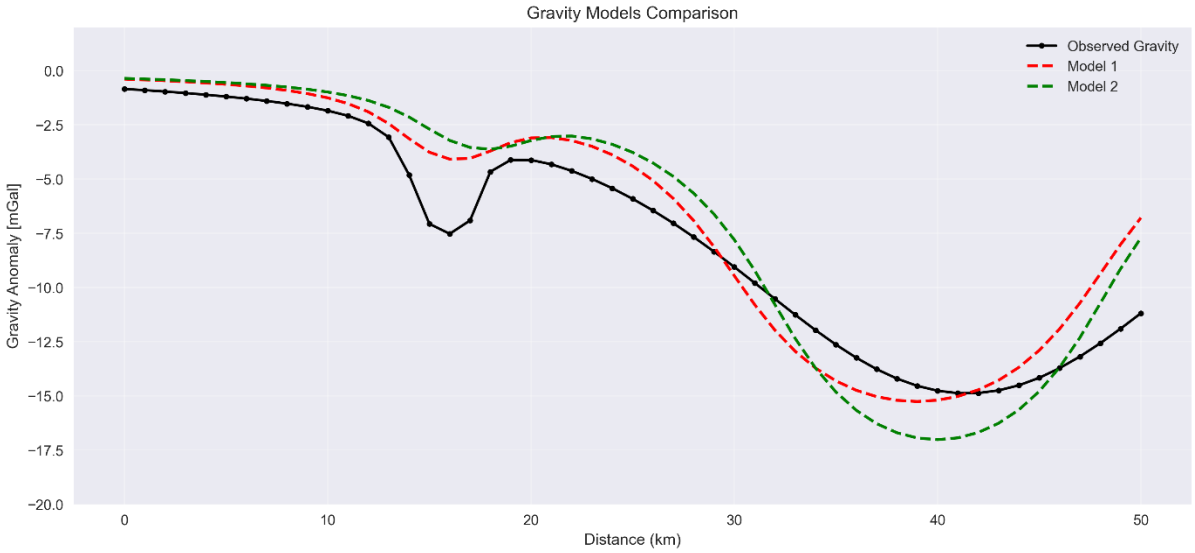

Figure 7. Gravity Models Comparison. Observed gravity anomaly (black) plotted against two forward models (Model 1 in red, Model 2 in green) along the 50 km survey line. Both synthetic profiles capture the broad shape of the anomaly, with Model 1 providing a closer fit in the central region and Model 2 better matching the deeper low around 40 km.

4.4 Magnetism Results

We built a block-based magnetic model using three subsurface bodies with assigned vertical magnetization. The model was used to calculate the vertical magnetic field component along the survey line.

The resulting synthetic profile was compared to the observed magnetic anomaly. The figure shows both data sets along the 50 kilometers profile. A root-mean-square (RMS) misfit of approximately 3.035 nT was calculated.

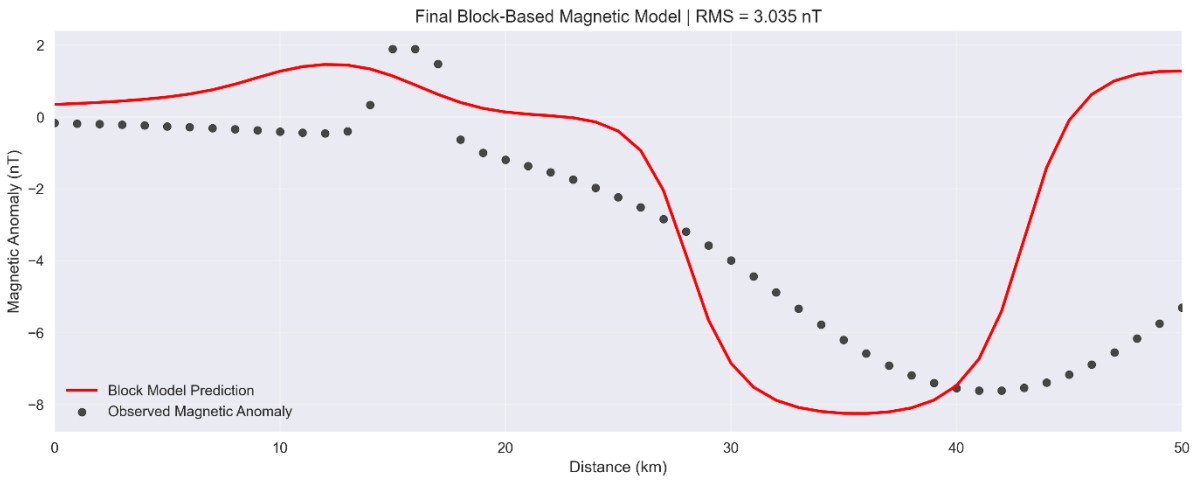

Figure 8. Observed vs. Modeled Magnetic Anomaly. Observed magnetic anomaly (black dots) compared with the block-based synthetic model (red line) along the survey line. The model captures the general shape of the anomaly with a root-mean-square (RMS) misfit of 3.035 nT.

5. Discussion

5.1 Interpretation of Seismic Data

The seismic results show five clear velocity layers. Wave speeds increase from about 2700 m/s near the surface to 6250 m/s at greater depths. The top four layers come from reflection data, and the deepest layer is based on refraction analysis. We did not see any direct wave arrivals.

The shallowest layer, at around 2700 m/s, likely matches sinter deposits seen at the surface near Biscuit Basin. Lab tests show sinter can have P-wave speeds as low as 2500 m/s, which supports this interpretation (Muñoz-Saez et al., 2016). The second and third layers are of velocities of approximately 3780 and 4710 m/s. These values are consistent with ignimbrites or lava flows which are common in the Yellowstone Plateau volcanic field. The sharp increase in velocity across these layers likely indicates transitions from porous rock to more consolidated material. The fourth layer of velocity of about 5400 m/s may represent welded volcanic rock. The deepest layer resolved by refraction data at 6250 m/s could be a dense crystalline basement. This velocity is consistent with mafic units or deep plutonic material that underlies the volcanic pile (Brown et al., 2009).

5.2 Interpretation of Gravity and Magnetics

The gravity results highlight two low-density zones. The first block between 14 and 18 kilometers lies at shallow depths between 1.5 and 4.0 kilometers. It likely reflects altered tuff or porous rhyolite near the surface. These rocks are common in Yellowstone's upper crust and are prone to hydrothermal overprinting (Fournier, 1989). The second larger anomaly block spans from 30 to 48 kilometers and extends from 2.5 to 9.5 kilometers depth. This broad feature suggests a sustained heating of rhyolitic units or even partial melting. Its strong magnetic low points to magnetite breakdown (Morgan et al., 2009).

The magnetic model includes three bodies. A weakly positive anomaly appears near 9 to 15 kilometers along the profile with a depth of 3 to 9 kilometers. This zone may represent remanent magnetization in less affected volcanic units. A small negative block from 17 to 27 kilometers and 4 to 8 kilometers deep likely reflects partial demagnetization from hydrothermal fluids. A much stronger negative anomaly block from 28 to 43 kilometers that extend to 14 kilometers depth points to a region of high heat.

Together, the gravity lows and magnetic lows overlap spatially beneath the explosion site. The use of both methods gives stronger evidence that high temperatures or fluids have modified the subsurface features.

5.3 Integrated Model: Single Interpretation

The geophysical results together support a model of a thermally active system beneath Biscuit Basin. Seismic velocities increase with depth, while gravity and magnetic lows align across the central profile. These patterns suggest a shallow zone of fluid circulation, underlain by a broader region of thermal alteration. The deepest anomalies may mark zones of past magmatic intrusion.

Overall, the data support a two-tier structure: a shallow hydrothermal system underlain by deeper magmatic influence. This should be the result of long-term heat transfer from below. The explosion site lies directly above this composite zone which reinforced the interpretation of ongoing subsurface activity.

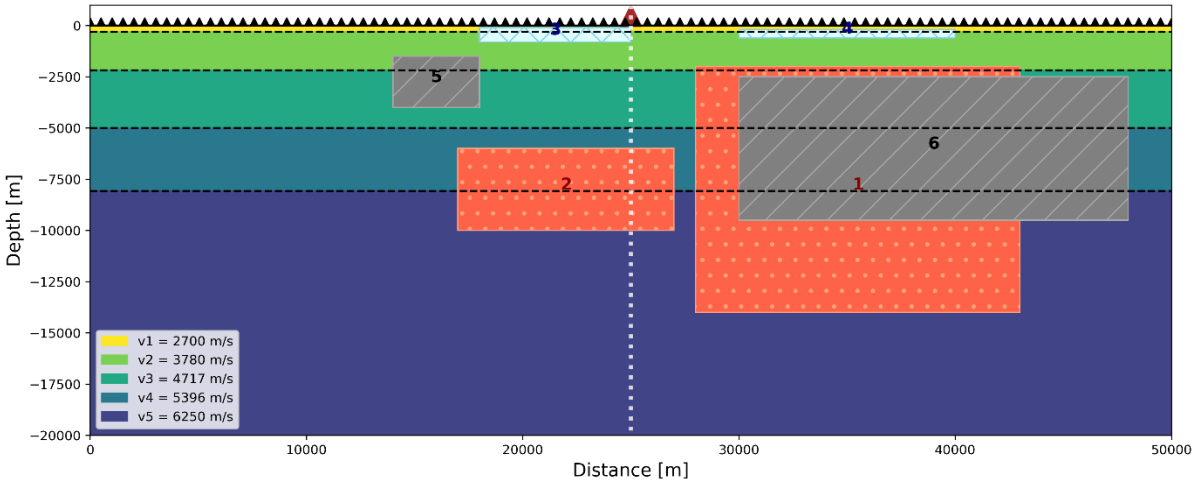

Figure 9. Complete Cross Section with Integrated Geophysical Features.

5.4 Sources of Error and Limitations

The main sources of error in this study are from simplified model geometry and assumptions. Seismic velocities were modeled using flat layers with constant velocities which may miss smaller features and it's not realistic. Gravity and magnetic models relied on block-based shapes which also cannot match realistic settings. Overlapping signals from different subsurface sources can also make it hard to isolate individual features. Noise, sparse sensor spacing, and the 2D nature of the model add further limitations. These factors can blur small features and make it harder to confidently locate subsurface structures. Future work with denser arrays and 3D modeling could improve resolution and reduce ambiguity.

5.5 Critical Thinking and Data Consistency

The three datasets together give a clearer view of the subsurface than any one method alone. Seismic data shows distinct layers with increasing wave speeds, while gravity and magnetic results highlight zones affected by heat. The gravity and magnetic lows overlap, suggesting thermal alteration.

These patterns don't always align perfectly, but that's expected. Heat and fluids can change rock density and magnetism without significantly affect wave speed. Overall, these datasets support the idea of a thermally active zone beneath Biscuit Basin and small differences between datasets may reveal areas where localized heat, fluids, or rock changes affect one physical property more than others.

6. Summary and conclusions

We used seismic, gravity and magnetic data to study the subsurface beneath Biscuit Basin. Seismic results revealed five velocity layers. Wave speeds increase from about 2700 m/s near the surface to 6250 m/s at depth. These changes outline different rock types, from surface sinter to deeper volcanic and basement material.

Gravity data showed two low-density zones. They likely formed where heat or fluids reduced the rock's density. Magnetic results included one small positive anomaly and two larger negative ones. The strongest magnetic low may mark a zone where high heat caused magnetite to break down.

The gravity and magnetic anomalies overlap beneath the explosion site. Seismic velocities also increase in this area, which may indicate more solid rock. When combined, the three datasets support a model with a shallow hydrothermal system above a deeper magmatic zone.

Using multiple datasets gives a clearer view of the subsurface. This approach helps us understand how heat and fluids shape the crust beneath Yellowstone. Future work should focus on adding more detailed measurements and expanding into three dimensions.

Reference

1. Morgan, L. A., Shanks, W. C., & Pierce, K. L. (2009).

Hydrothermal processes above the Yellowstone magma chamber: Large hydrothermal systems and large hydrothermal explosions. Geological Society of America Special Paper 459. https://doi.org/10.1130/2009.2459(01)

2. Fournier, R. O. (1989).

Geochemistry and dynamics of the Yellowstone National Park hydrothermal system. Annual Review of Earth and Planetary Sciences, 17(1), 13–53. https://doi.org/10.1146/annurev.ea.17.050189.000305

3. Muñoz-Saez, C., Saltiel, S., Manga, M., Nguyen, C., & Gonnermann, H. (2016).

Physical and hydraulic properties of modern sinter deposits: El Tatio, Atacama. Journal of Volcanology and Geothermal Research, 323, 14–28.

10.1016/j.jvolgeores.2016.06.026

4. Brown, D., Llana-Funez, S., Carbonell, R., Alvarez-Marron, J., Marti, D., & Salisbury, M. (2009). Laboratory measurements of P-wave and S-wave velocities across a surface analog of the continental crust–mantle boundary: Cabo Ortegal, Spain. *Earth and Planetary Science Letters*, 279(3–4), 223–233. https://doi.org/10.1016/j.epsl.2009.05.032